Published in final edited form as:
Circulation. 2009 September 15; 120(11 0): S238–S246. doi:10.1161/CIRCULATIONAHA.109.885236.

Stem Cells for Myocardial Repair With Use of a Transarterial Catheter

Xiaohong Wang, MD, PhD, **Mohammad Nurulqadr Jameel, MD**, **Qinglu Li, BS**, **Abdul Mansoor, MD, PhD**, **Xiong Qiang, MS**, **Cory Swingen, PhD**, **Carmelo Panetta, MD**, and **Jianyi Zhang, MD, PhD**
Department of Medicine, University of Minnesota Medical School, Minneapolis, Minn

Abstract

Background—Using a swine model of postinfarction left ventricle (LV) remodeling, we investigated marrow-derived, multipotent progenitor cell (MPC) transplantation into hearts with acute myocardial infarction (AMI) via a novel transarterial catheter.

Methods and Results—The left anterior descending coronary artery was balloon-occluded after percutaneous transluminal angiography to generate AMI (60-minute no-flow ischemia). The transarterial catheter was then placed in the same coronary artery, and either 50×10^6 MPCs (cell group, n=6) or saline (control, n=6) was injected into the border zone (BZ) myocardium. LV function was assessed by magnetic resonance imaging before AMI and at 1 and 4 weeks after AMI, whereas myocardial energy metabolism was assessed by ^{31}P-magnetic resonance spectroscopy at week 4. One week after AMI, the ejection fraction was significantly reduced in both groups from a baseline of ≈50% to 31.3±3.9% (cell group) and 33.3±3.1% (control). However, at week 4, the cell group had a significant recovery in ejection fraction. The functional improvements were accompanied by a significant improvement in myocardial bioenergetics. Histologic data demonstrated a 0.55% cell engraftment rate 4 weeks after MPC transplantation. Only 2% of engrafted cells were costaining positive for cardiogenic markers. Vascular density in the BZ was increased in the cell group. Conditioned medium from cultured MPCs contained high levels of vascular endothelial growth factor, which was increased in response to hypoxia. MPCs cocultured with cardiomyocytes inhibited changes in cardiomyocyte mitochondrial membrane potential and cytochrome *c* release induced by tumor necrosis factor-α.

Conclusions—Thus, a paracrine effect may contribute significantly to the observed therapeutic effects of MPC transplantation.

Keywords

stem cells; metabolism; myocardial infarct

Stem cell transplantation has emerged as a novel therapeutic strategy for limiting postinfarction left ventricular (LV) remodeling and the consequent development of

Correspondence to Jianyi Zhang, MD, PhD, University of Minnesota Health Science Center, Mayo Mail Code 508, 420 Delaware St SE, Minneapolis, MN 55455. zhang047@umn.edu.
The first 2 authors contributed equally to this article.

Presented in part at American Heart Association Scientific Sessions 2008, November 8–12, 2008, New Orleans, La.

The online-only Data Supplement is available with this article at http://circ.ahajournals.org/cgi/content/full/120/11_suppl_1/S238/DC1.

Disclosures: None.

congestive heart failure in both animal[1–4] and clinical[5–9] studies. Using a swine model of post–myocardial infarction (MI) LV remodeling, we recently reported that transplantation of bone marrow–derived, multipotent progenitor cells (MPCs) resulted in a significant improvement of cardiac function and correction of abnormal energy metabolism.[1] However, the mechanisms underlying these beneficial effects are not well defined. We and others have demonstrated a very low engraftment rate and an even lower cardiomyocyte differentiation rate a few weeks after bone marrow stem cell transplantation.[1,10] Therefore, the direct contribution of regenerated myocytes to the improved cardiac contractile function appears less likely. The group of Dzau and colleagues[10–12] has shown a significant protection of stressed cardiomyocytes from apoptosis and a consequent reduction in infarct size by injection of concentrated cell culture medium that was obtained from bone marrow–derived mesenchymal stem cells (MSCs) with overexpression of Akt, or by injection of MSCs themselves into the myocardium at the time of acute MI. More recently, they demonstrated that the frizzled related protein 2 is the key paracrine factor secreted by Akt-modified MSCs that mediates myocardial survival and repair.[13] Using a swine model of concentric LV hypertrophy (LVH), we have demonstrated that transplantation of vascular endothelial growth factor (VEGF)–overexpressing MSCs at the time of ascending aortic banding markedly attenuated the development of LVH and resulted in the preservation of LV contractile performance and bioenergetic characteristics,[14] supporting the notion that the beneficial effects after bone marrow stem cell transplantation are mediated through a paracrine mechanism by secretion of trophic factors from stem cells that exert a protective effect.

Many different approaches have been used to deliver stem cells into the heart, including direct intramyocardial, intravenous, intracoronary, and retrograde coronary venous routes.[15] Intracoronary infusion of stem cells at the time of angiography seems the most practical approach clinically. However, its efficacy and safety remain an issue. In a canine model, it was reported that coronary artery infusion of stem cells resulted in blockage of small vessels, which in turn caused discrete micromyocardial necrosis.[16] The Microsyringe infusion catheter (Mercator MedSystems) used in the present study has the unique feature of a microneedle that penetrates the coronary artery wall and allows the user to inject the stem cells directly into the myocardium.

The present study had a 2-fold hypothesis. First, we hypothesized that MPC delivery via the Micro-syringe infusion catheter would be safe and effective in a clinically relevant porcine model of myocardial ischemia/reperfusion. Second, we hypothesized that a trophic effect plays an important role in mediating the myocardial structural changes that lead to the beneficial effects of cellular therapy. Namely, the engrafted cells release cytokines that result in enhanced angiogenesis, maintenance of mitochondrial integrity, and inhibition of apoptosis of ischemia-threatened and overstretched myocytes in the border zone (BZ) myocardium adjacent to the myocardial infarct. These structural changes are accompanied by an improvement of BZ myocardial contractile performance, which in turn results in ameliorating the LV wall stress and myocardial bioenergetics.

Methods

All experiments were performed in accordance with the animal use guidelines of the University of Minnesota, and the experimental protocol was approved by the University of Minnesota research animal resources committee. The investigation conformed to the *Guide for the Care and Use of Laboratory Animals* published by the National Institutes of Health (NIH publication No. 85-23, revised 1985).

Cell Culture

MPCs were provided by Athysis, Inc, which were derived from 1 of the male swine multipotent adult progenitor cell lines generated at the University of Minnesota.[17] MPC isolation, expansion, and differentiation were performed as described previously[1] and are described in detail in the online-only data supplement.

Myocardial Ischemia/Reperfusion Model and Transarterial Stem Cell Injection

Young Yorkshire female swine (≈20 kg; Manthei Hog Farm, Elk River, Minn) were anesthetized with pentobarbital (30 mg/kg IV), intubated, and ventilated with a respirator with supplemental O_2. Left heart catheterization was performed. MI was created by balloon occlusion of the left anterior descending coronary artery (LAD) distal to the second diagonal for 60 minutes followed by reperfusion after anticoagulation. The transarterial catheter (Microsyringe infusion catheter from Mercator MedSystems) was then placed in the same coronary artery, and either stem cells (50×10^6/mL; n=6) or saline (n=6) was injected. The intramyocardial position of the needle was confirmed under fluoroscopy in the cardiac catheterization laboratory with contrast diluted for both placebo and cell injection to confirm delivery outside the vessel lumen. Five equal injections for a total of 50×10^6 MPCs were given, with a final volume of 1 mL. When ventricular fibrillation occurred, electric defibrillation was performed immediately. Animals received standard postoperative care, including analgesia, until they ate normally and became active.

MRI Methods

Animals were examined at baseline, 1 week after MI, and then 4 weeks after MI by magnetic resonance imaging (MRI). MRI was performed on a 1.5-T clinical scanner (Siemens Sontata, Siemens Medical Systems, Islen, NJ) with a phased-array 4-channel surface coil and ECG gating. Details of the MRI methods are described in the data supplement.

^{1}H-NMR Spectroscopy and Spatially Localized ^{31}P-NMR Spectroscopy Technique

Animals were returned to the laboratory for a final open-chest MR spectroscopic study 4 weeks after MI. The ^{1}H-nuclear (N) MR and ^{31}P-NMR spectroscopy techniques are described in detail in the data supplement.

Surgical Preparation for Open-Chest MR Spectroscopy Study

Detailed surgical preparations for the MR spectroscopy study have been published previously[1,18,19] and are described in the data supplement.

MR Spectroscopy Study Protocol and Hemodynamic Measurements

Hemodynamic measurements were acquired simultaneously with the NMR spectra. Aortic and LV pressures were measured with pressure transducers positioned at midchest level[19–21] and recorded on an 8-channel recorder. After all of the baseline data were obtained, animals received a combined dobutamine and dopamine infusion (20 μg/kg per min each) to induce a very high cardiac work state. After an ≈5-minute wait after the initiation of catecholamine infusion, all of the spectroscopic and hemodynamic data were again measured under the high cardiac work state.

Tissue Preparation

The LV was sectioned in a bread-loaf manner into 6 transverse sections (≈10 mm in thickness) from apex to base. Even rings were subdivided into 12 circumferential specimens

and fixed in zinc fixative (Anatech Ltd, Battle Creek, Mich) for hematoxylin and eosin staining, immunofluorescence staining, and engraftment evaluation.

Engraftment Evaluation

Each of the 12 pieces of cardiac tissue of a short-axis ring was stained with X-gal (Invitrogen) and embedded in Tissue-Tek OCT (Fisher Scientific). Serial cryostat sections (10 μm in thickness) were obtained from the whole transverse even rings. Engrafted MPCs were identified by counting the X-gal–positive nuclei in every tenth serial section of the whole transverse ring and then multiplying by 10 to obtain the total number of engrafted MPCs per ring. The total number of engrafted MPCs equals 2-fold the number of X-gal–positive staining cells in all 3 even rings. The engraftment rate of transplanted MPCs was calculated by dividing the total number of engrafted MPCs by 50×10^6 (the number of MPCs injected) and multiplying by 100%.

Immunohistochemistry

Detailed immunohistochemistry methods have been described previously.[14,22] In brief, cryostat sections (10-μm thickness) were obtained for immunofluorescence staining to evaluate myocyte or endothelial differentiation of injected cells. Antibodies used included troponin T (cardiac isoform Ab-1; Laboratory Vision Corp, Chicago, Ill) and α-sarcomeric actin, N-cadherin, and CD31 (Research Diagnostic, Inc, Flanders, NJ). Nuclear counterstaining was performed with 4′,6′-diamino-2-phenylindole (DAPI, Molecular Probes, Grand Island, NY).

Analysis of Myocardial Vascular Density

Vascular density was assessed by staining with anti-CD31 (BD Biosciences, San Diego, Calif) antibody. The sections were visualized by fluorescence-labeled secondary antibody (Molecular Probes, Inc, Eugene, Ore). Images were taken at a magnification of 20× with an Olympus microscope (BX51/BX52, Tokyo). The number of capillaries was counted in a blinded fashion in 3 fields per section of the peri-infarct zone, and a total of 5 sections per ring were analyzed (n=4 for each group). The quality of the computer analysis (Image J) was checked against manual counting.

HL-1 Myocyte Culture and Apoptosis

HL-1 myocytes (from Claycomb Laboratory, University of Louisiana) were cultured as previously described.[14] In brief, HL-1 cells were plated onto fibronectin-gelatin-coated plates or flasks and cultured in Claycomb medium supplemented with 10% fetal bovine serum, 100 U/mL penicillin, 100 μg/mL streptomycin, 0.1 mmol/L norepinephrine, and 2 mmol/L L-glutamine. For the coculture experiment, HL-1 cells were plated in 12-well plates at a total density of 5×10^5 (1:3 ratio of MPCs to HL-1 cells) in half MPC medium and half Claycomb medium. Before being cocultured, HL-1 cells were labeled with Vybrant CFDA SE cell tracer kit (Molecular Probes). Labeled HL-1 cells were extensively washed and cocultured with MPCs. The coculture and HL-1 cells alone were treated with 40 ng tumor necrosis factor (TNF)-α for 18 hours. Apoptosis was assessed by staining with Hoechst 33342 (H33342) dye and then quantifying the percentage of apoptotic nuclei (300 cells counted per sample) in the CFDA-labeled subset by identifying cells with H33342 staining.[14]

Identification of Angiogenic Factors Released From Stem Cells

The cultured MPCs were divided into 2 subgroups (5×10^4cells per group). One MPC group was exposed to 2% O_2 (hypoxia). The other group was cultured under normoxic conditions. Eighteen hours later, the unconcentrated supernatants were subjected to ELISA for VEGF

and insulin-like growth factor (IGF) content according to the respective manufacturer's instructions.

Detection of Changes in Mitochondrial Membrane Potential (Δψm)

HL-1 cells were plated on chamber slides, and the next day, cells were stained with H33342 dye. After being thoroughly washed 3 times, MPCs were plated onto the chamber slides (1:1 ratio). After 12 hours, the cells were treated with 40 ng TNF-α for 6 hours. Mitochondrial inner-membrane-potential changes were evaluated with a mitochondria staining kit according to the manufacturer's directions (Sigma-Aldrich, St. Louis, Mo). The cationic, lipophilic dye, JC-1 (5,5′,6,6′-tetrachloro-1,1′,3,3′-tetraethylbenzimidazolo-carbocyanine iodide), aggregates can be visualized in the mitochondria as bright red fluorescence, representing intact mitochondria, and JC-1 monomers can be visualized as green fluorescence, which represents disrupted mitochondria.

MPCs Cocultured With Neonatal Cardiomyocytes and Cytochrome *c* Release

Primary cultures of cardiac myocytes were prepared by enzymatic digestion of ventricles obtained from neonatal (2-day-old) Sprague-Dawley rats as previously described.[22] Coculture experiments were established in the fibronectin-coated chamber slides at a total density of 2×10^4 (1:1 ratio of cardiomyocytes to MPCs) in MPC medium supplemented with 2% fetal bovine serum, 100 μg/mL penicillin, and 250 μg/mL streptomycin at 37°C in humid air with 5% CO_2. Cytochrome *c* release was detected by immunofluorescence staining with an anti–cytochrome *c* antibody after cardiomyocytes and the coculture cells were treated with 40 ng TNF-α. Troponin T was used to stain cardiomyocytes. Double-staining cardiomyocytes were detected and counted.

Statistics and Data Analysis

Anatomic data, wall stress data, capillary density, and the in vitro apoptosis data were compared between the 2 groups (MI and MI+ cells) with Student's *t* test. A repeated-measures ANOVA was applied to compare the measurements of systolic thickening fraction, ejection fraction (EF), and scar size across the 2 treatment groups (MI and MI+ cells) and different time points (before MI and 1 and 4 weeks after MI) and to compare the measurement of myocardial phosphocreatine (PCr)/ATP and hemodynamic data across the 2 treatment groups (MI and MI+ cells) and 2 hemodynamic conditions (baseline and after inotropic stimulation). For comparison between the 2 treatment groups, the conventional significance level of a type I error ($P<0.05$) was used. The Bonferroni correction for significance level was used to take into account multiple comparisons. All values are expressed as mean±SD. All statistical analyses were performed in Sigmastat version 3.5 (San Jose, Calif).

Statement of Responsibility

The authors had full access to the data and take responsibility for its integrity. All authors have read and agree to the manuscript as written.

Results

Anatomic and Hemodynamic Data

Four of the 16 pigs with LAD occlusion and reperfusion died within the first 60 minutes after coronary occlusion due to ventricular fibrillation. The surviving 12 pigs were randomized to receive either MPCs (n=6) or saline only (n=6). The anatomic data for the 12 swine with LAD ligation is summarized in supplemental Table I. The degree of LVH as reflected by LV weight/body weight and right ventricle weight/body weight was not

significantly different between the MPC and saline groups. The hemodynamic data at baseline and at increased workload are summarized in supplemental Table II. Inotropic stimulation caused a significant increase in heart rate and LV systolic pressure and consequently, the rate-pressure product. However, there was no significant difference between the swine with cell treatment and those without cell treatment.

Global Functional Data

The temporal changes in global function as measured by MRI are depicted in Figure 1. There was no significant difference between the 2 groups at baseline. At week 1, the distal LAD occlusion caused a similar scar size in both groups, with a significant decrease in LVEF, with no significant difference between the 2 groups. However, there was remarkable LV chamber functional recovery from 1 week to 4 weeks after cell transplantation (EF, 46.3±6.6% versus 33.3±3.1%, $P<0.001$), which was not observed in the control group (Figure 1A). Thus, at week 4, LVEF was significantly higher in cell-treated animals than in control animals (46.3±6.6% versus 35.4±3.2%, $P<0.001$; Figure 1A). This functional improvement in the MPC treatment group was accompanied by a significant decrease in scar size at 4 weeks compared with the saline group (4.8±1.9% versus 8.8±2.1%, $P=0.047$). It should be noted that there was a significant decrease in scar size from week 1 to week 4 in the cell-treated group (4.8±1.9% at 4 weeks versus 9.2±3.5% at 1 week, $P<0.001$; Figure 1B).

Regional Contractile Functional Data

The LV was divided into 16 segments. The apex was divided into 4, the mid-LV into 6, and the base into 6 segments. Distal LAD occlusion resulted in a thin-walled infarct in the apex, mainly in the anteroseptal segments (segments 1 and 2). The remaining apical segments (segments 3 and 4) are the BZ, and the mid-LV and base make up the remote zone. Systolic thickening fraction was measured as a surrogate marker of regional LV contractile function. Distal LAD occlusion alone resulted in systolic bulging of the infarct zone at 1 week, which persisted to 4 weeks (Table). MPC treatment resulted in an increased systolic thickening fraction of the infarct and BZ at 4 weeks compared with control (Table). Moreover, the systolic thickening fraction in the infarct and BZ within cell-treated animals was significantly increased at 4 weeks compared with 1 week (Table). LV wall stress (σ) in different LV segments at 4 weeks was calculated according to the Laplace law, as previously described, from the following equation: $\sigma = PR/(2T)$,[23] where P is LV pressure, R is chamber radius, and T is wall thickness measured from cine MRI images in the particular region of the LV. MPC treatment resulted in a significant decrease in wall stress in the infarct (300 ± 16 mm Hg in control versus 208 ±20 mm Hg in MPC-treated animals, $P=0.009$) and BZ (242±18 mm Hg in control versus 174± 14 mm Hg in MPC-treated animals, $P=0.01$).

Myocardial High-Energy Phosphate and Inorganic Phosphate Levels

Myocardial high-energy phosphate and inorganic phosphate levels are reflected by the PCr-ATP ratios as shown in Figure 2. The PCr-ATP ratio was significantly higher at 4 weeks in the pigs treated with MPCs compared with those without such treatment (2.03±0.31 versus 1.53±0.28, $P=0.009$). After increased workload, the PCr-ATP ratio decreased in both groups but was still significantly higher in the cell-treated pigs (1.80±0.24 versus 1.43±0.25, $P=0.027$). No deoxymyoglobin resonance peak was detected in either group by ^{1}H-NMR spectroscopy, which supports our previous finding that the BZ bioenergetic abnormalities in hearts with postinfarction LV remodeling are not caused by persistent myocardial ischemia.

Cell Engraftment and Differentiation In Vivo

Cell engraftment was determined by counting β-galactosidase-staining positive cells in tissue sections, and the cell engraftment rate was calculated as a percentage of engrafted cells from the total 50×10^6 injected stem cells. Two additional pigs were euthanized at 10 days after MI and cell transplantation to assess engraftment at an earlier time. Ten days after cell transplantation, the cell engraftment rate was ≈5%. Most of the cells were retained in the infarcted area, and only a small portion of the engrafted cells resided in the peri-infarct and remote areas (Figure 3A). Four weeks after cell transplantation, the cell engraftment rate was remarkably decreased and reached 0.55% (n=6). To determine the differentiation of engrafted cells, tissue sections were double-stained for ß-galactosidase and cardiac-specific markers, including troponin T, α-sarcomeric actin, and N-cadherin. We found that ≈2% of engrafted cells costained positive for ß-galactosidase and troponin T or α-sarcomeric actin 10 days after cell transplantation (Figures 3B and 3C). These double-staining positive cells were only observed in the peri-infarct and remote areas. Among the cells that costained positive for ß-galactosidase or α-sarcomeric actin, we identified gap junctions between the cells, as indicated by N-cadherin immunofluorescence staining (Figure 3B). These data suggest that transplanted MPCs engraft successfully and can undergo in vivo transdifferentiation into cardiomyocyte-like cells or form fused cells.

Vascular Density

To determine the mechanisms underlying the beneficial effects of MPC transplantation, we investigated the effects of MPC transplantation on neovascularization and angiogenesis in the post-MI hearts. At 4 weeks after cell transplantation, immunofluorescence staining for CD31 antibody indicated significant angiogenesis in stem cell–treated hearts, with more CD31-expressing capillaries being present in peri-infarct regions of cell-treated compared with saline-treated hearts (Figure 4A). Quantitative evaluation of CD31-positive capillary numbers per high-power field (20×) indicated that vascular density was significantly greater in the MPC-treated group than in the saline-treated group (Figures 4A and 4B). However, few cells stained positive for both the endothelial cell marker CD31 and ß-galactosidase (data not shown). These data suggest that transplanted MPCs may promote angiogenesis through a paracrine effect.

To further identify the angiogenic factors, we determined the levels of VEGF and IGF in the conditioned medium under different culture conditions. We found that MPCs can secrete detectable VEGF under normoxic condition, which was significantly increased in response to hypoxia (normoxia, 456.1±104.1 pg/5×10^4 cells; hypoxia, 1543.8±77.1 pg/5×10^4cells, n=5, $P<0.001$). However, the IGF levels secreted under both conditions were too low to be detected. These data suggest that MPCs secrete VEGF, which is an important angiogenic factor contributing to the observed cellular therapy–associated beneficial effects.

Protective Effect of MPCs on Mitochondrial Membrane Potential

To investigate the protective effect of MPCs on cardiomyocytes, HL-1 myocyte apoptosis was induced by inflammatory factor TNF-α. Coculture of HL-1 cells with MPCs significantly inhibited TNF-α–induced apoptosis (HL-1+TNF-α, 32±3%; TNF-α+coculture, 14±1%, n=6, $P<0.001$; Figure 5A). To further determine its underlying mechanisms, the alteration in mitochondrial inner-membrane electrochemical potential was determined by staining with the cationic, lipophilic dye, JC-1. MPCs significantly inhibited TNF-α–induced HL-1 cell mitochondrial membrane potential changes (Figure 5B). Cocultured MPCs with neonatal cardiomyocytes also inhibited TNF-α–induced cytochrome *c* release from neonatal cardiomyocytes (Figure 5C). These data suggest that the paracrine factors secreted by MPCs play a protective role in preventing myocytes from apoptosis.

Discussion

The present study demonstrates that MPC transplantation through a transcoronary arterial catheter approach is safe, feasible, and effective. MPC transplantation is associated with increase in vascular density, inhibition of apoptosis, and reduction of infarct size, which is accompanied by improvement in BZ and infarct zone contractile function and consequent improvement in myocardial bioenergetics and global LV function. These functional beneficial effects were observed despite low engraftment of MPCs at 4 weeks. In vitro, the MPCs significantly inhibited TNF-α–induced mitochondrial membrane potential changes and cytochrome *c* release from myocytes. Additionally, coculture of MPCs with HL-1 cells inhibited TNF-α–induced apoptosis. Thus, the MPC-induced trophic effect results in structural changes that are characterized by increased vascular density, spared myocytes from apoptosis, and decreased infarct size, which in turn lead to an improvement of BZ myocardial contractile performance, amelioration of regional wall stress, and myocardial bioenergetics.

Stem Cell Delivery Via Transarterial Injection

Although clinical trials of intracoronary artery infusion of stem cells have shown moderate LV functional improvement,[5,7–9] a report of a dog study suggested that coronary artery infusion of stem cells resulted in blockage of small vessels, which in turn caused discrete micromyocardial necrosis.[16] In the present study, we used a transarterial catheter with a microneedle that penetrates the coronary artery wall and injects stem cells directly into the myocardium that is exposed to ischemia/reperfusion. We found similar engraftment of stem cells as in previous studies of open-heart direct intramyocardial injection.[1,24] These data demonstrate that transcoronary injection of MPCs through this technique is safe and leads to an improvement in LV function.

Contractile Performance in the Infarct BZ

Increased LV wall stress in the BZ has been implicated among the factors contributing to LV remodeling after MI.[18,25] It has been shown in a porcine model that MI leads to dyskinesis in the infarct region and hypokinesis in the infarct BZ.[18] MPC transplantation caused an improvement in infarct and BZ systolic thickening fraction in the present study (Table), which in turn effectively reduced wall stress (BZ wall stress was 242±18 mm Hg in control versus 174±14 mm Hg in MPC-treated animals, P=0.01) and consequently improved the mismatch of energy delivery and demand (Figure 2).[1,24] The contractile performance improvement in the BZ is likely based on the myocardial structural improvements that are characterized by increased vascular density (Figure 4) and reduced apoptosis (Figure 5) in the BZ and myocyte differentiation (Figure 3).

BZ Myocardial Energetics

Postinfarction LV remodeling is associated with decreased high-energy phosphates, PCr-ATP ratio, and expression of several proteins crucial to oxidative ATP production, and these abnormalities are most severe in the BZ.[18] Our study confirmed these reports and showed that these abnormalities are worsened during a catecholamine stimulation-induced high cardiac work state (Figure 2). The improved myocardial bioenergetics in response to stem cell transplantation was also supported by the in vitro experiments indicating that mitochondrial inner-membrane electrochemical potential was significantly improved (Figure 5B), which could effectively increase the mitochondrial oxidative phosphorylation potential. This improvement in mitochondrial function may have an important role in cell survival and inhibition of the apoptotic pathway in resident cardiac progenitors.

Effect of Cell Transplantation on Infarct Size

Sequential MRI functional assessment allowed us to conclude that the infarct size in swine treated with MPCs decreased from week 1 to week 4, whereas scar sizes in swine without MPC treatment were maintained throughout follow-up (Figure 1B). This reduction in scar size with stem cell treatment has been noted in other reports.[2,12] The beneficial effects of MPC transplantation could be related to MPC differentiation into cardiomyocytes[26] or mobilization of endogenous progenitors to the injury site by paracrine effects.[12] Recently, it has been shown that endogenous cardiac progenitor cells, on activation, can home to the infarcted myocardium and help in myocardial regeneration.[27–30] In the present study, <1% of transplanted MPCs were engrafted at 4 weeks, and even a smaller percentage expressed markers of cardiomyocytes. This suggests that the functional and bioenergetic improvements are likely secondary to paracrine effects. The data from the present study indicate a trophic effect; ie, the cytokines released from the engrafted stem cells act on the host myocytes and spare them from apoptosis.

Stem Cell–Induced Antiapoptosis Effect

Apoptosis does occur in failing hearts.[31] Mitochondrial release of cytochrome *c* has been implicated in apoptosis induced by TNF-α.[32] MSC transplantation has been shown to have significant antiapoptosis effects.[4,11,12] Data from the present study support this hypothesis and further elucidate this finding by showing that MPCs cocultured with neonatal rat cardiomyocytes inhibit TNF-α–induced cytochrome *c* release. Mitochondria play a central role in apoptotic pathways. It has been shown that the mitochondrial respiratory chain complex I is inhibited in the early phase of TNF-α–induced apoptosis.[32] Inhibition of complex I can affect electron flow through the other complexes of mitochondrial oxidative phosphorylation leading to cytochrome *c* release and caspase-3 activation, followed by a reduction of mitochondrial membrane potential. The data from the present study demonstrate that the TNF-α–induced loss of mitochondrial membrane potential can be inhibited by stem cell treatment. The improvement in myocardial energetics in vivo with MPC treatment observed in the present study indicates that the impairment in the mitochondrial respiratory chain, F0F1 ATP synthase, and ATP production is ameliorated by MPC treatment.

Stem Cell–Induced Neovascularization

We hypothesized that the mechanism for improvement in ventricular function in response to MPC transplantation is partially due to neovascularization. MPC-treated animals demonstrated a significant increase in vascular density compared with animals that received saline (Figure 4). This generation of new coronary vessels after ischemic injury is very important clinically, as it leads to increased blood flow to the infarct and BZ[33] and consequently spares ischemia-threatened myocytes from apoptosis, leading to improved ventricular function. The neovascularization is probably related to an increase in both angiogenesis and vasculogenesis. Previously, we reported that vasculogenesis as evidenced by endothelial differentiation from MPCs did contribute to the increased vascular density, although only 3% of the engrafted MPCs differentiated into endothelial cells.[1] In our present study, we observed insignificant endothelial differentiation of transplanted MPCs 4 weeks after cell transplantation. Thus, it seems that the endothelial differentiation from MPCs has a minimal effect on vasculogenesis. However, it is possible that MPC transplantation results in recruitment of endogenous cardiac or bone marrow endothelial progenitor cells that leads to vasculogenesis and contributes to the increased vascular density (Figure 4B). In addition, it has been recently demonstrated that transplantation of cardiac progenitor cells induces neovascularization primarily through vasculogenesis.[33] Data from the present study demonstrate that MPCs secrete a significant level of VEGF under normoxic conditions,

which was further increased in response to hypoxia. It has been previously reported that VEGF secretion by MSCs is a potent angiogenic factor that promotes neovascularization as well as inhibits apoptosis.[34] Taken together, these data demonstrate that VEGF plays an important role in myocardial protection that is associated with MPC transplantation.

In summary, the present study demonstrates that transcoronary artery injection of MPCs in a porcine model of ischemia/reperfusion resulted in improvement of myocardial contractile function, reduction of BZ wall stress, limitation of scar size expansion, and balance of myocardial energy delivery and demand. Because the engraftment rate was low and myogenic differentiation was even lower, the beneficial effects are most likely related to the trophic effects of MPCs on the host myocardium, which include promotion of angiogenesis, maintenance of mitochondrial integrity, and inhibition of apoptosis of ischemia-threatened and overstretched myocytes in the BZ myocardium.

Supplementary Material

Refer to Web version on PubMed Central for supplementary material.

Acknowledgments

Both MPCs and Microsyringe infusion catheters (from Mercator MedSystems), were gifts kindly provided by Athysis, Inc. The rat neonatal cardiomyocytes were kindly provided by John Fassett.

Sources of Funding: This work was supported by US Public Health Service grants HL50470, HL 67828, and HL95077. X.W. was supported by American Heart Association grant-in-aid No. 0750160Z. M.N.J. was supported by American Heart Association Greater Midwest Predoctoral Award No. 0810015Z.

References

1. Zeng L, Hu Q, Wang X, Mansoor A, Lee J, Feygin J, Zhang G, Suntharalingam P, Boozer S, Mhashilkar A, Panetta CJ, Swingen C, Deans R, From AH, Bache RJ, Verfaillie CM, Zhang J. Bioenergetic and functional consequences of bone marrow–derived multipotent progenitor cell transplantation in hearts with postinfarction left ventricular remodeling. Circulation. 2007; 115:1866–1875. [PubMed: 17389266]
2. Amado LC, Saliaris AP, Schuleri KH, St John M, Xie JS, Cattaneo S, Durand DJ, Fitton T, Kuang JQ, Stewart G, Lehrke S, Baumgartner WW, Martin BJ, Heldman AW, Hare JM. Cardiac repair with intramyocardial injection of allogeneic mesenchymal stem cells after myocardial infarction. Proc Natl Acad Sci U S A. 2005; 102:11474–11479. [PubMed: 16061805]
3. Linke A, Muller P, Nurzynska D, Casarsa C, Torella D, Nascimbene A, Castaldo C, Cascapera S, Bohm M, Quaini F, Urbanek K, Leri A, Hintze TH, Kajstura J, Anversa P. Stem cells in the dog heart are self-renewing, clonogenic, and multipotent and regenerate infarcted myocardium, improving cardiac function. Proc Natl Acad Sci U S A. 2005; 102:8966–8971. [PubMed: 15951423]
4. Mangi AA, Noiseux N, Kong D, He H, Rezvani M, Ingwall JS, Dzau VJ. Mesenchymal stem cells modified with Akt prevent remodeling and restore performance of infarcted hearts. Nat Med. 2003; 9:1195–1201. [PubMed: 12910262]
5. Assmus B, Honold J, Schachinger V, Britten MB, Fischer-Rasokat U, Lehmann R, Teupe C, Pistorius K, Martin H, Abolmaali ND, Tonn T, Dimmeler S, Zeiher AM. Transcoronary transplantation of progenitor cells after myocardial infarction. N Engl J Med. 2006; 355:1222–1232. [PubMed: 16990385]
6. Assmus B, Schachinger V, Teupe C, Britten M, Lehmann R, Dobert N, Grunwald F, Aicher A, Urbich C, Martin H, Hoelzer D, Dimmeler S, Zeiher AM. Transplantation of Progenitor Cells and Regeneration Enhancement in Acute Myocardial Infarction (TOPCARE-AMI). Circulation. 2002; 106:3009–3017. [PubMed: 12473544]
7. Janssens S, Dubois C, Bogaert J, Theunissen K, Deroose C, Desmet W, Kalantzi M, Herbots L, Sinnaeve P, Dens J, Maertens J, Rademakers F, Dymarkowski S, Gheysens O, Van Cleemput J,

Bormans G, Nuyts J, Belmans A, Mortelmans L, Boogaerts M, Van de Werf F. Autologous bone marrow-derived stem-cell transfer in patients with ST-segment elevation myocardial infarction: double-blind, randomised controlled trial. Lancet. 2006; 367:113–121. [PubMed: 16413875]

8. Schachinger V, Erbs S, Elsasser A, Haberbosch W, Hambrecht R, Holschermann H, Yu J, Corti R, Mathey DG, Hamm CW, Suselbeck T, Assmus B, Tonn T, Dimmeler S, Zeiher AM. Intracoronary bone marrow-derived progenitor cells in acute myocardial infarction. N Engl J Med. 2006; 355:1210–1221. [PubMed: 16990384]
9. Wollert KC, Meyer GP, Lotz J, Ringes-Lichtenberg S, Lippolt P, Breidenbach C, Fichtner S, Korte T, Hornig B, Messinger D, Arseniev L, Hertenstein B, Ganser A, Drexler H. Intracoronary autologous bone-marrow cell transfer after myocardial infarction: the BOOST randomised controlled clinical trial. Lancet. 2004; 364:141–148. [PubMed: 15246726]
10. Noiseux N, Gnecchi M, Lopez-Ilasaca M, Zhang L, Solomon SD, Deb A, Dzau VJ, Pratt RE. Mesenchymal stem cells overexpressing Akt dramatically repair infarcted myocardium and improve cardiac function despite infrequent cellular fusion or differentiation. Mol Ther. 2006; 14:840–850. [PubMed: 16965940]
11. Gnecchi M, He H, Liang OD, Melo LG, Morello F, Mu H, Noiseux N, Zhang L, Pratt RE, Ingwall JS, Dzau VJ. Paracrine action accounts for marked protection of ischemic heart by Akt-modified mesenchymal stem cells. Nat Med. 2005; 11:367–368. [PubMed: 15812508]
12. Gnecchi M, He H, Noiseux N, Liang OD, Zhang L, Morello F, Mu H, Melo LG, Pratt RE, Ingwall JS, Dzau VJ. Evidence supporting paracrine hypothesis for Akt-modified mesenchymal stem cell-mediated cardiac protection and functional improvement. FASEB J. 2006; 20:661–669. [PubMed: 16581974]
13. Mirotsou M, Zhang Z, Deb A, Zhang L, Gnecchi M, Noiseux N, Mu H, Pachori A, Dzau V. Secreted frizzled related protein 2 (Sfrp2) is the key Akt-mesenchymal stem cell-released paracrine factor mediating myocardial survival and repair. Proc Natl Acad Sci USA. 2007; 104:1643–1648. [PubMed: 17251350]
14. Wang X, Hu Q, Mansoor A, Lee J, Wang Z, Lee T, From AH, Zhang J. Bioenergetic and functional consequences of stem cell-based VEGF delivery in pressure-overloaded swine hearts. Am J Physiol. 2006; 290:H1393–H1405.
15. Perin EC, Lopez J. Methods of stem cell delivery in cardiac diseases. Nat Clin Pract Cardiovasc Med. 2006; 3(suppl 1):S110–S113. [PubMed: 16501616]
16. Vulliet PR, Greeley M, Halloran SM, MacDonald KA, Kittleson MD. Intra-coronary arterial injection of mesenchymal stromal cells and microinfarction in dogs. Lancet. 2004; 363:783–784. [PubMed: 15016490]
17. Zeng L, Rahrmann E, Hu Q, Lund T, Sandquist L, Felten M, O'Brien TD, Zhang J, Verfaillie C. Multipotent adult progenitor cells from swine bone marrow. Stem Cells. 2006; 24:2355–2366. [PubMed: 16931778]
18. Hu Q, Wang X, Lee J, Mansoor A, Liu J, Zeng L, Swingen C, Zhang G, Feygin J, Ochiai K, Bransford TL, From AH, Bache RJ, Zhang J. Profound bioenergetic abnormalities in peri-infarct myocardial regions. Am J Physiol. 2006; 291:H648–H657.
19. Ye Y, Gong G, Ochiai K, Liu J, Zhang J. High-energy phosphate metabolism and creatine kinase in failing hearts: a new porcine model. Circulation. 2001; 103:1570–1576. [PubMed: 11257087]
20. Zhang J, McDonald KM. Bioenergetic consequences of left ventricular remodeling. Circulation. 1995; 92:1011–1019. [PubMed: 7641336]
21. Zhang J, Merkle H, Hendrich K, Garwood M, From AH, Ugurbil K, Bache RJ. Bioenergetic abnormalities associated with severe left ventricular hypertrophy. J Clin Invest. 1993; 92:993–1003. [PubMed: 8349829]
22. Wang X, Hu Q, Nakamura Y, Lee J, Zhang G, From AH, Zhang J. The role of the sca-1+/CD31- cardiac progenitor cell population in postinfarction left ventricular remodeling. Stem Cells. 2006; 24:1779–1788. [PubMed: 16614004]
23. Feygin J, Hu Q, Swingen C, Zhang J. Relationships between regional myocardial wall stress and bioenergetics in hearts with left ventricular hypertrophy. Am J Physiol. 2008; 294:H2313–H2321.

24. Feygin J, Mansoor A, Eckman P, Swingen C, Zhang J. Functional and bioenergetic modulations in the infarct border zone following autologous mesenchymal stem cell transplantation. Am J Physiol. 2007; 293:H1772–H1780.
25. Guccione JM, Moonly SM, Moustakidis P, Costa KD, Moulton MJ, Ratcliffe MB, Pasque MK. Mechanism underlying mechanical dysfunction in the border zone of left ventricular aneurysm: a finite element model study. Annals Thorac Surg. 2001; 71:654–662.
26. Rota M, Kajstura J, Hosoda T, Bearzi C, Vitale S, Esposito G, Iaffaldano G, Padin-Iruegas ME, Gonzalez A, Rizzi R, Small N, Muraski J, Alvarez R, Chen X, Urbanek K, Bolli R, Houser SR, Leri A, Sussman MA, Anversa P. Bone marrow cells adopt the cardiomyogenic fate in vivo. Proc Natl Acad Sci U S A. 2007; 104:17783–17788. [PubMed: 17965233]
27. Bearzi C, Rota M, Hosoda T, Tillmanns J, Nascimbene A, De Angelis A, Yasuzawa-Amano S, Trofimova I, Siggins RW, Lecapitaine N, Cascapera S, Beltrami AP, D'Alessandro DA, Zias E, Quaini F, Urbanek K, Michler RE, Bolli R, Kajstura J, Leri A, Anversa P. Human cardiac stem cells. Proc Natl Acad Sci U S A. 2007; 104:14068–14073. [PubMed: 17709737]
28. Rota M, Padin-Iruegas ME, Misao Y, De Angelis A, Maestroni S, Ferreira-Martins J, Fiumana E, Rastaldo R, Arcarese ML, Mitchell TS, Boni A, Bolli R, Urbanek K, Hosoda T, Anversa P, Leri A, Kajstura J. Local activation or implantation of cardiac progenitor cells rescues scarred infarcted myocardium improving cardiac function. Circ Res. 2008; 103:107–116. [PubMed: 18556576]
29. Urbanek K, Rota M, Cascapera S, Bearzi C, Nascimbene A, De Angelis A, Hosoda T, Chimenti S, Baker M, Limana F, Nurzynska D, Torella D, Rotatori F, Rastaldo R, Musso E, Quaini F, Leri A, Kajstura J, Anversa P. Cardiac stem cells possess growth factor-receptor systems that after activation regenerate the infarcted myocardium, improving ventricular function and long-term survival. Circ Res. 2005; 97:663–673. [PubMed: 16141414]
30. Urbanek K, Torella D, Sheikh F, De Angelis A, Nurzynska D, Silvestri F, Beltrami CA, Bussani R, Beltrami AP, Quaini F, Bolli R, Leri A, Kajstura J, Anversa P. Myocardial regeneration by activation of multipotent cardiac stem cells in ischemic heart failure. Proc Natl Acad Sci U S A. 2005; 102:8692–8697. [PubMed: 15932947]
31. Olivetti G, Abbi R, Quaini F, Kajstura J, Cheng W, Nitahara JA, Quaini E, Di Loreto C, Beltrami CA, Krajewski S, Reed JC, Anversa P. Apoptosis in the failing human heart. N Engl J Med. 1997; 336:1131–1141. [PubMed: 9099657]
32. Higuchi M, Proske RJ, Yeh ET. Inhibition of mitochondrial respiratory chain complex I by TNF results in cytochrome *c* release, membrane permeability transition, and apoptosis. Oncogene. 1998; 17:2515–2524. [PubMed: 9824162]
33. Tillmanns J, Rota M, Hosoda T, Misao Y, Esposito G, Gonzalez A, Vitale S, Parolin C, Yasuzawa-Amano S, Muraski J, De Angelis A, Lecapitaine N, Siggins RW, Loredo M, Bearzi C, Bolli R, Urbanek K, Leri A, Kajstura J, Anversa P. Formation of large coronary arteries by cardiac progenitor cells. Proc Natl Acad Sci U S A. 2008; 105:1668–1673. [PubMed: 18216245]
34. Tang YL, Zhao Q, Zhang YC, Cheng L, Liu M, Shi J, Yang YZ, Pan C, Ge J, Phillips MI. Autologous mesenchymal stem cell transplantation induce VEGF and neovascularization in ischemic myocardium. Regulatory Peptides. 2004; 117:3–10. [PubMed: 14687695]

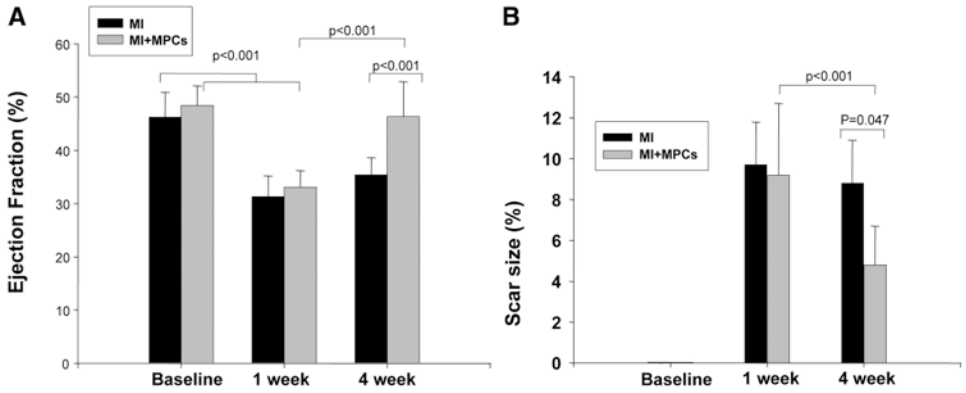

Figure 1.

The functional and structural improvements 4 weeks after MPC transplantation into MI hearts. A, MPC transplantation into the BZ myocardium in a swine ischemia/reperfusion model significantly attenuated the deterioration of cardiac function. B, MPC transplantation into the BZ myocardium in a swine ischemia/reperfusion model significantly limited scar size expansion after MI at 4 weeks. Data are mean±SD, n=6 in each group. Pairwise probability values were derived from repeated-measures ANOVA with Bonferroni correction.

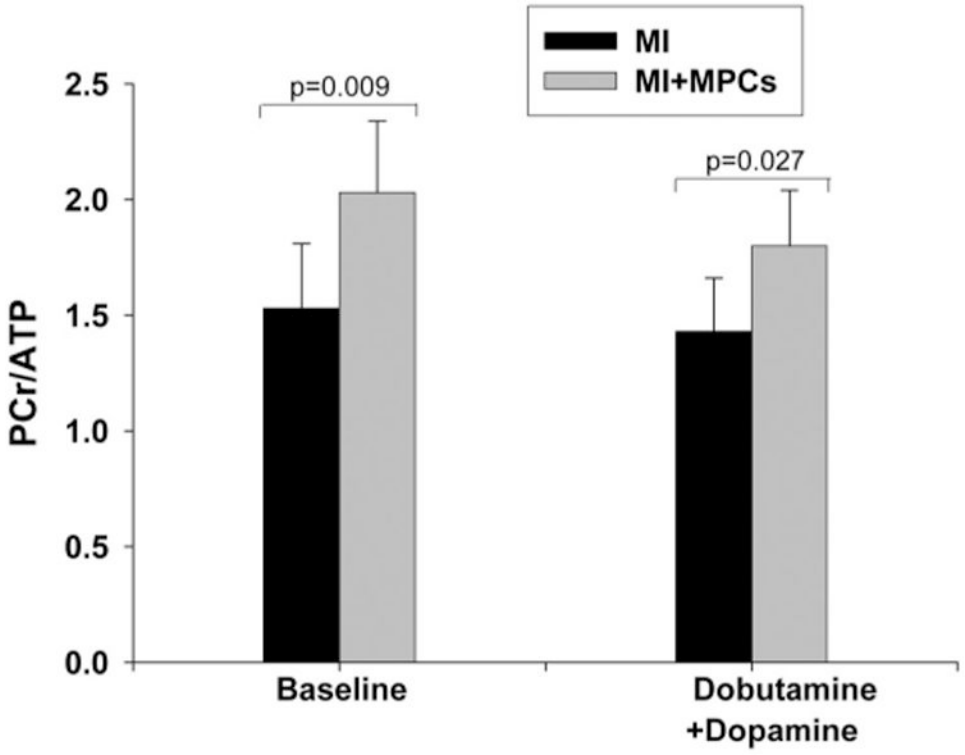

Figure 2.
MPC transplantation into the BZ myocardium significantly improved LV bioenergetics, as reflected by altered myocardial PCr/ATP 4 weeks after MI at baseline and in high work states. Data are mean±SD, n=6 in each group. Pairwise probability values were derived from repeated-measures ANOVA with Bonferroni correction.

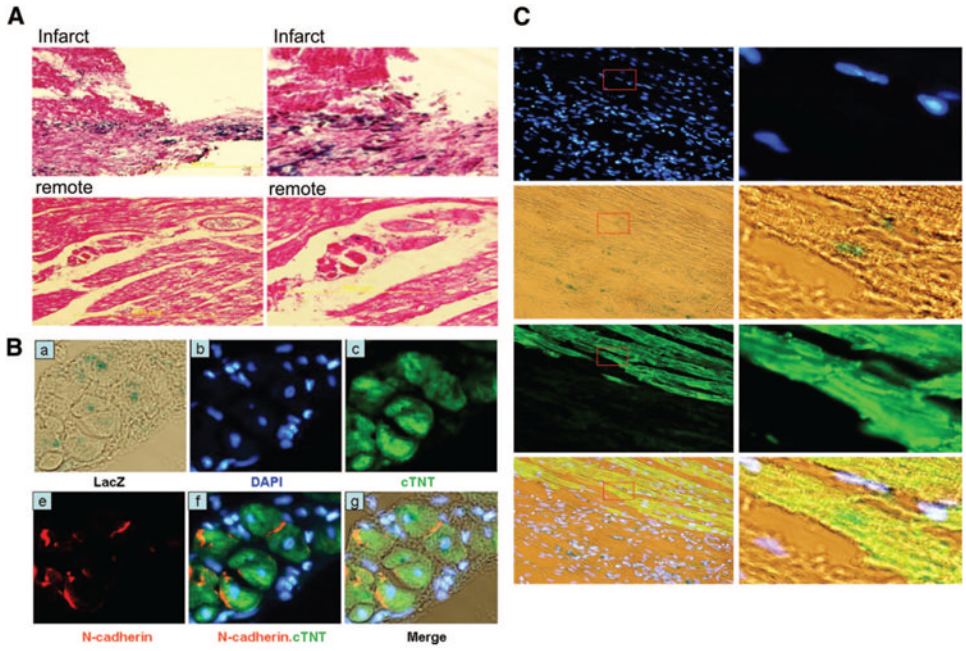

Figure 3.

Histologic staining of tissues from the heart 10 days after transplantation of retrovirus LacZ-labeled swine MPCs. A, Hematoxylin-eosin staining of tissues from the heart 10 days after transplantation of retrovirus LacZ-labeled swine MPCs. Panel a shows that the engrafted cells (LacZ) are distributed in peri-infarct and remote regions (magnification ×100); panel (b) shows the same sections at high magnification (magnification ×400). B, Engraftment and differentiation of swine MPCs in vivo. Swine MPCs labeled with LacZ were injected into MI hearts via transmural catheter delivery, and the tissues were harvested and dissected into 10-μm sections. Dissected samples were stained for LacZ (dark blue), troponin T (green), and/or N-cadherin (red). Nuclei were stained with DAPI (blue). Upper panel, low magnification; lower panel, high magnification. C, Engraftment and differentiation of swine MPCs in vivo. Dissected samples were stained for LacZ (blue) and α-sarcomeric actin (green). Nuclei were stained with DAPI (blue). Left panel, low magnification; right panel, high magnification.

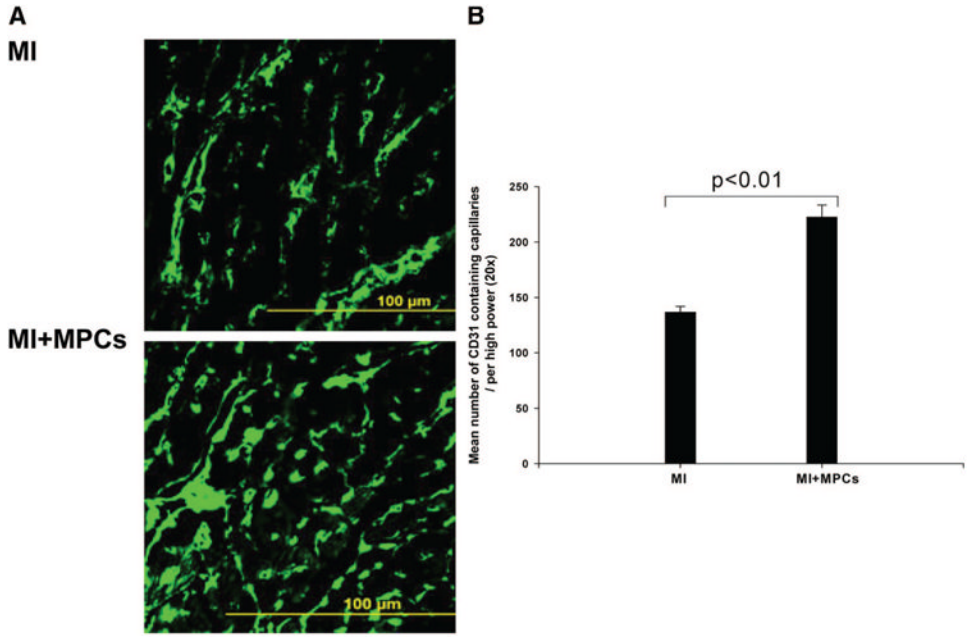

Figure 4.

Transplantation of MPCs into MI hearts significantly promoted angiogenesis, which was probably mediated by release of VEGF. A, Immunofluorescence staining of tissues from MI and MPC transplantation heart; B, Mean number of CD31-containing capillaries in the BZ myocardium (n=6, $P<0.01$). Data are mean±SD.

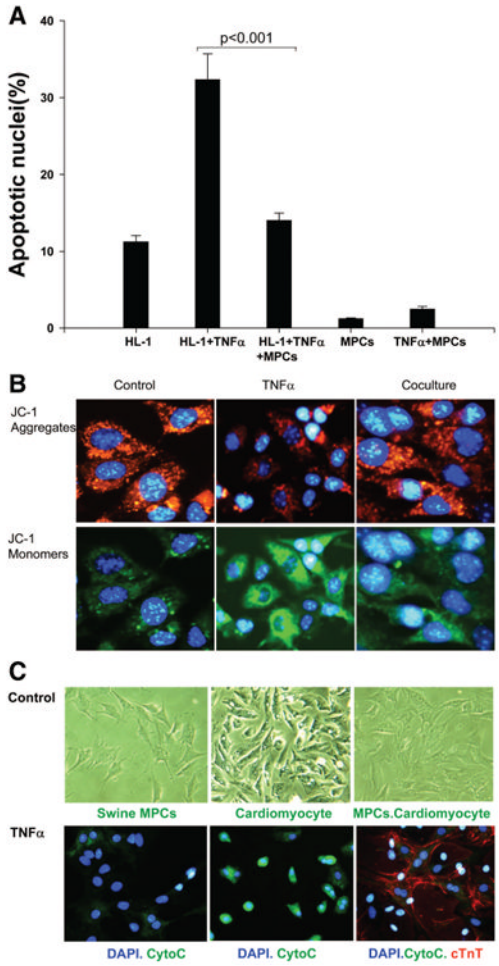

Figure 5.

The protective effect of MPCs on cardiomyocytes. A, Cocultured swine MPCs and HL-1 cells significantly inhibited TNF-*α*–induced HL-1 cell apoptosis (n=6, $P<0.001$). Data are mean±SD. B, Swine MPCs cocultured with HL-1 cells significantly inhibited TNF-*α*–induced mitochondrial membrane potential changes. C, Swine MPCs cocultured with rat neonatal cardiomyocytes significantly inhibited TNF-*α*–induced cytochrome *c* release.

Table

Systolic Thickening Fraction 1 and 4 Weeks After MI, Measured by MRI

	Infarct Zone			BZ			Remote Zone		
	1 Week	4 Weeks	*P* Value Within Group	1 Week	4 Weeks	*P* Value Within Group	1 Week	4 Weeks	*P* Value Within Group
MI	−4.3±1.5	−4.5±1.3	0.927	8.9±1.4	8.8±1.7	0.986	27.9±3.0	30.9±5.7	NS
MI+ Cells	1.0±3.9	17.3±2.9	<0.001	12.3±2.8	24.1 ±5.5	0.005	28.7±4.6	34.2±4.9	NS
P value between groups	0.031	<0.001		0.229	<0.001		NS	NS	

Values are mean±SD; n=6 in each group; Pairwise *P* values were derived from repeated-measures ANOVA with Bonferroni correction. NS indicates not significant.